

# Cross sections of inclusive $\psi(2S)$ and $X(3872)$ production from $b$ -hadron decays in $pp$ collisions and comparison with ATLAS and CMS data

B. A. Kniehl<sup>1</sup>, G. Kramer<sup>1</sup>, I. Schienbein<sup>2</sup> and H. Spiesberger<sup>3</sup>

<sup>1</sup> II. Institut für Theoretische Physik, Universität Hamburg,  
Luruper Chaussee 149, D-22761 Hamburg, Germany

<sup>2</sup> Laboratoire de Physique Subatomique et de Cosmologie,  
Université Joseph Fourier Grenoble 1,  
CNRS/IN2P3, Institut National Polytechnique de Grenoble,  
53 avenue des Martyrs, F-38026 Grenoble, France

<sup>3</sup> PRISMA<sup>+</sup> Cluster of Excellence, Institut für Physik, Johannes-Gutenberg-Universität,  
Staudinger Weg 7, D-55099 Mainz, Germany,

March 2, 2021

## Abstract

We study the cross sections for the inclusive production of  $\psi(2S)$  and  $X(3872)$  hadrons in  $pp$  collisions at the LHC at two different center-of-mass energies and compare with experimental data obtained by the ATLAS, CMS, and LHCb collaborations.

PACS: 12.38.Bx, 12.39.St, 13.85.Ni, 14.40.Nd

# 1 Introduction

Some time ago, Paolo Bolzoni and two of us calculated the cross section for the inclusive production of  $J/\psi$  and  $\psi(2S)$  mesons originating from decays of  $B$  mesons produced in  $p\bar{p}$  collisions with center-of-mass energy  $\sqrt{S} = 1.96$  TeV at the Fermilab Tevatron and in  $pp$  collisions with  $\sqrt{S} = 7$  TeV at the CERN LHC at next-to-leading order (NLO) in the framework of the general-mass variable-flavor number scheme (GM-VFNS) in connection with nonrelativistic-QCD (NRQCD) factorization [1]. In Ref. [1], the transverse momentum ( $p_T$ ) distributions of such non-prompt  $J/\psi$  mesons measured by the CDF II [2, 3], CMS [4, 5], LHCb [6, 7], ATLAS [8], and ALICE [9] collaborations were found to be very well described by our predictions, with respect to both absolute normalization and line shape. Similarly, the  $p_T$  distributions of  $\psi(2S)$  non-prompt production measured by CDF II [3], CMS [5], and LHCb [7] were rather well described by our calculations.

In 2003, a narrow charmonium-like state was discovered in exclusive  $B^+ \rightarrow J/\psi K^+ \pi^+ \pi^-$  decays by the BELLE collaboration [10]. The subsequent development was described in detail in publications by CMS [11] and ATLAS [12], where the first measurements of  $X(3872)$  at the LHC were reported, and in two review articles [13, 14].

In 2017, ATLAS published measurements of the  $\psi(2S)$  and  $X(3872)$  cross sections in  $pp$  collisions at  $\sqrt{S} = 8$  TeV, both for prompt and non-prompt production [12]. Both, the  $\psi(2S)$  and  $X(3872)$  hadrons were detected via their decays to  $J/\psi \pi^+ \pi^-$ . The experimental results for prompt production were found to be in agreement with predictions of nonrelativistic QCD (NRQCD) factorization [15, 16, 17]. The  $\psi(2S)$  non-prompt production cross section was compared with FONLL predictions [18] and also found to agree very well with the ATLAS data [12].

Also the cross section of  $X(3872)$  non-prompt production measured by ATLAS [12] was compared with theory. Specifically, the non-prompt  $\psi(2S)$  production cross section evaluated in the FONLL scheme was rescaled by the ratio of branching fractions

$$R_B = \frac{\text{Br}(B \rightarrow X(3872) + X) \text{Br}(X(3872) \rightarrow J/\psi \pi^+ \pi^-)}{\text{Br}(B \rightarrow \psi(2S) + X) \text{Br}(\psi(2S) \rightarrow J/\psi \pi^+ \pi^-)}, \quad (1)$$

which was evaluated using the result  $\text{Br}(B \rightarrow X(3872) + X) \text{Br}(X(3872) \rightarrow J/\psi \pi^+ \pi^-) = (1.9 \pm 0.8) \times 10^{-4}$  extracted in Ref. [19] from Tevatron data [20] and values  $\text{Br}(B \rightarrow \psi(2S) + X) = (3.07 \pm 0.21) \times 10^{-3}$  and  $\text{Br}(\psi(2S) \rightarrow J/\psi \pi^+ \pi^-) = 0.3446 \pm 0.0030$  quoted by the Particle Data Group [21] to give

$$R_B^{\text{Tev}} = 0.18 \pm 0.08. \quad (2)$$

This led to an overestimation of the ATLAS data by a large factor, increasing with  $p_T$  from about 4 to about 8 [12].

We observe that the value of  $R_B$  in Eq. (2) is a factor of 5 larger than the one measured by ATLAS in a two-lifetime fit [12],

$$R_B^{2L} = (3.57 \pm 0.348) \times 10^{-2}. \quad (3)$$

If this lower value had been used instead of the larger value based on Ref. [19], the differential cross section  $d\sigma/dp_T$  of  $X(3872)$  non-prompt production calculated in the FONLL framework would have been in approximate agreement with the ATLAS measurement [12]. We are not aware of an explanation for the discrepancy between the two values of  $R_B$ .

The  $\psi(2S)$  and  $X(3872)$  processes considered here differ in the mechanisms of both production from  $B$ -hadron decay and decay to  $J/\psi\pi^+\pi^-$ . The  $\psi(2S)$  meson is a pure  $c\bar{c}$  state, whereas the  $X(3872)$  hadron is believed to be a quantum mechanical mixture of the pure  $c\bar{c}$  state  $\chi_{1c}(2P)$  and a  $D^0\bar{D}^{*0}$  molecule, which is predominantly produced via its  $\chi_{1c}(2P)$  component [15, 16, 17]. These differences are reflected in the fact that  $R_B$  is so different from unity. The value of  $R_B$  could be predicted from purely theoretical considerations, *e.g.*, on the basis of effective field theories derived from QCD in combination with hadron models. However, this would reach beyond the scope of this work. Instead, we adopt here a more heuristic approach to  $R_B$  based on the interpretation of experimental data.

In the present work, we shall present the results of an alternative calculation of  $d\sigma/dp_T$  for  $\psi(2S)$  non-prompt production in the kinematic range relevant for the ATLAS measurements [12], based on the GM-VFNS. The calculation of  $d\sigma/dp_T$  for a fixed rapidity ( $y$ ) range was described in detail in Ref. [1], which is based on the earlier analysis [22] based on the zero-mass variable-flavor-number scheme (ZM-VFNS), where bottom is included among the massless quark flavors. An alternative GM-VFNS approach, in the SACOT- $m_T$  scheme, was described in Ref. [23], but cross sections of  $J/\psi$  or  $\psi(2S)$  production have not yet been calculated in that scheme.

## 2 Results

We start by considering  $\psi(2S)$  non-prompt hadroproduction. Its theoretical treatment in the GM-VFNS was described in Ref. [1]. Without any additional assumptions, we thus obtain the results for the differential cross section  $d\sigma/dp_T$  at  $\sqrt{S} = 8$  TeV, averaged over the rapidity range  $|y| < 0.75$ , which are presented for  $10 < p_T < 70$  GeV in Fig. 1(a) and compared with the ATLAS data [12]. We adopt the choices of renormalization and (unified) factorization scales,  $\mu_R$  and  $\mu_F$ , from our recent analysis of  $B^\pm$ -meson hadroproduction at the LHC [24] by setting  $\mu_R = \xi\mu_T$  and  $\mu_F = 0.49\mu_T$ , with  $\mu_T = \sqrt{p_T^2 + 4m_b^2}$  and  $m_b = 4.5$  GeV, and varying  $\xi$  between 0.5 and 2 about its default value 1 to estimate the theoretical uncertainty. We use set CT14nlo [25] of parton distribution functions (PDFs) and the  $B$ -meson fragmentation functions (FFs) from Ref. [26]. As in the ATLAS analysis [12], we include the  $B^+$ ,  $B_s^0$ , and  $\Lambda_b^0$  hadrons and their antiparticles [27] taking into account the respective  $b \rightarrow B$ -hadron branching fractions as given in Ref. [21]. Here, we selected the ATLAS data set corresponding to the long-lifetime contribution determined by the two-lifetime fit, where the short-lifetime contribution is attributed to the  $B_c \rightarrow \psi(2S) + X$  decay. The data corresponding to the one-lifetime fit are quite similar, except that the cross sections in the first two  $p_T$  bins are slightly larger. We observe from Fig. 1(a) that the agreement between experiment and theory is quite good, except for the upmost  $p_T$  bin.

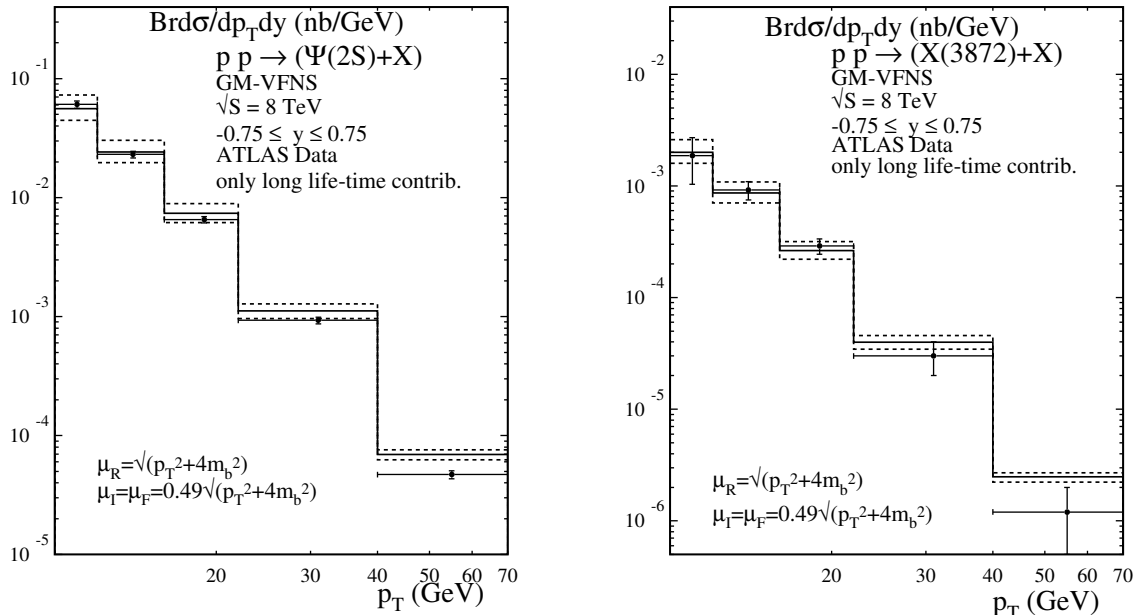


Figure 1: Double differential cross sections times branching fractions for (a)  $\psi(2S)$  (left) and (b)  $X(3872)$  (right) non-prompt hadroproduction at  $\sqrt{S} = 8$  TeV, averaged over  $y$  in the region  $|y| \leq 0.75$ , as a function of  $p_T$ . The solid points with error bars represent the ATLAS data [12]. The solid and the upper and lower dashed histograms represent our NLO GM-VFNS predictions for  $\xi = 1, 0.5, 2$ , respectively.

We now turn to  $X(3872)$  non-prompt hadroproduction. We convert our results for  $\psi(2S)$  non-prompt hadroproduction shown in Fig. 1(a) to the  $X(3872)$  case by including the  $R_B^{2L}$  ratio listed in Eq. (3). In Fig. 1(b), we compare the outcome with the respective ATLAS data, again for the two-lifetime fit [12]. The ATLAS data for the single-lifetime fit are somewhat larger in the first two  $p_T$  bins. We emphasize that the value of  $R_B^{2L}$  in Eq. (3) comes from the same experimental analysis as the cross sections  $d\sigma/dp_T$  of inclusive  $\psi(2S)$  and  $X(3872)$  production, albeit from a different observable, namely from the ratio of long-lived  $X(3872)$  to long-lived  $\psi(2S)$  production rates with additional information from the  $p_T$  dependencies (see Fig. 4(b) in Ref. [12]). Of course, one would like to have this information also from an independent experiment, for example from  $\psi(2S)$  and  $X(3872)$  production in  $e^+e^-$  annihilation. Unfortunately such information is not available yet.

The quality of agreement between data and theoretical predictions is similar for  $\psi(2S)$  and  $X(3872)$  production. It would be interesting to perform a comparative analysis of  $\psi(2S)$  and  $X(3872)$  production in  $e^+e^-$  annihilation. After all, the  $R_B$  ratio should not depend on the production mechanism.

Our results for  $X(3872)$  non-prompt hadroproduction shown in Fig. 1(b) were obtained

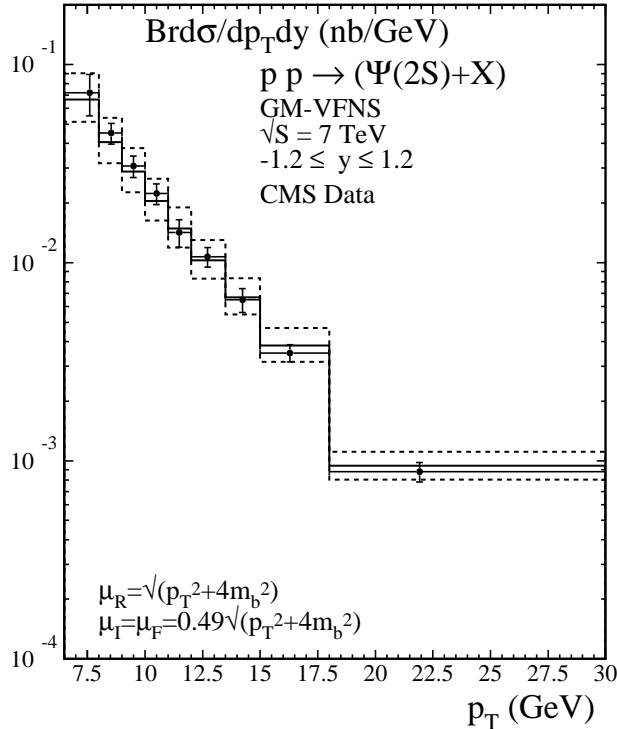


Figure 2: Double differential cross section times branching fraction for  $\psi(2S)$  non-prompt hadroproduction at  $\sqrt{S} = 7$  TeV, averaged over  $y$  in the region  $|y| \leq 1.2$ , as a function of  $p_T$ . The solid points with error bars represent the CMS data [5]. The solid and the upper and lower dashed histograms represent our NLO GM-VFNS predictions for  $\xi = 1, 0.5, 2$ , respectively.

using the value of  $R_B^{2L}$  given in Eq. (3). To obtain a cross-check, we determine  $R_B$  by fitting our theory prediction to the ATLAS data [12] for the five  $p_T$  bins, assuming Gaussian errors. We thus obtain

$$R_B^{\text{ATLAS}} = \left( 3.41 \pm 0.37 \begin{array}{c} +0.63 \\ -0.56 \end{array} \right) \times 10^{-2}, \quad (4)$$

where the first error is propagated from the experimental data and the second errors are due to the uncertainty of the theory prediction from  $\xi$  variations as explained above. This value agrees within errors with the value given in Eq. (3) obtained from the two-lifetime fit in Ref. [12]. Its central value is slightly smaller and its error somewhat larger than in Eq. (3). We conclude that the determinations of  $R_B$  from the two-lifetime fit and from the cross section analyses by ATLAS are consistent with each other.

To obtain yet another check of our assumption that the  $R_B$  value in Eq. (3) [12] is realistic, we use it for a comparison with the inclusive cross section  $d\sigma/dp_T$ , integrated over  $|y| < 1.2$ , of non-prompt  $X(3872)$  production measured by the CMS collaboration at  $\sqrt{S} = 7$  TeV [11]. In Ref. [11], this cross section was not reported directly, but it can be calculated in four  $p_T$  bins from the prompt  $X(3872)$  cross section times branching ratio (Table 7 in Ref. [11])

and the  $X(3872)$  non-prompt fraction (Table 6 in Ref. [11]). Since both measurements have rather large uncertainties, the same is true also for the non-prompt cross section, but this should be sufficient for the sake of an approximate cross-check. In Ref. [11], CMS used as a benchmark their earlier measurement of the inclusive cross section of non-prompt  $\psi(2S)$  production, also at  $\sqrt{S} = 7$  TeV and for  $|y| < 1.2$ , but with a different  $p_T$  binning [5]. In Ref. [1], we compared these data with our prediction, which came as a continuous function in  $p_T$ . We now repeat this comparison adopting the very  $p_T$  binning from Ref. [5] and present the outcome in Fig. 2. The good agreement, which is evident from Fig. 2, reassures us of that our prediction of non-prompt  $\psi(2S)$  production serves as a useful starting point for generating a prediction of non-prompt  $X(3872)$  production.

We thus proceed by adjusting the  $p_T$  binning according to Ref. [11] and including the  $R_B$  value from Eq. (3). In Fig. 3(a), the outcome is compared with the inclusive cross section of non-prompt  $X(3872)$  production extracted from Ref. [11] as explained above. We find satisfactory agreement within the rather large experimental errors, albeit not as good as for the ATLAS data [12] in Fig. 1(b). However, our predictions do not deviate more than

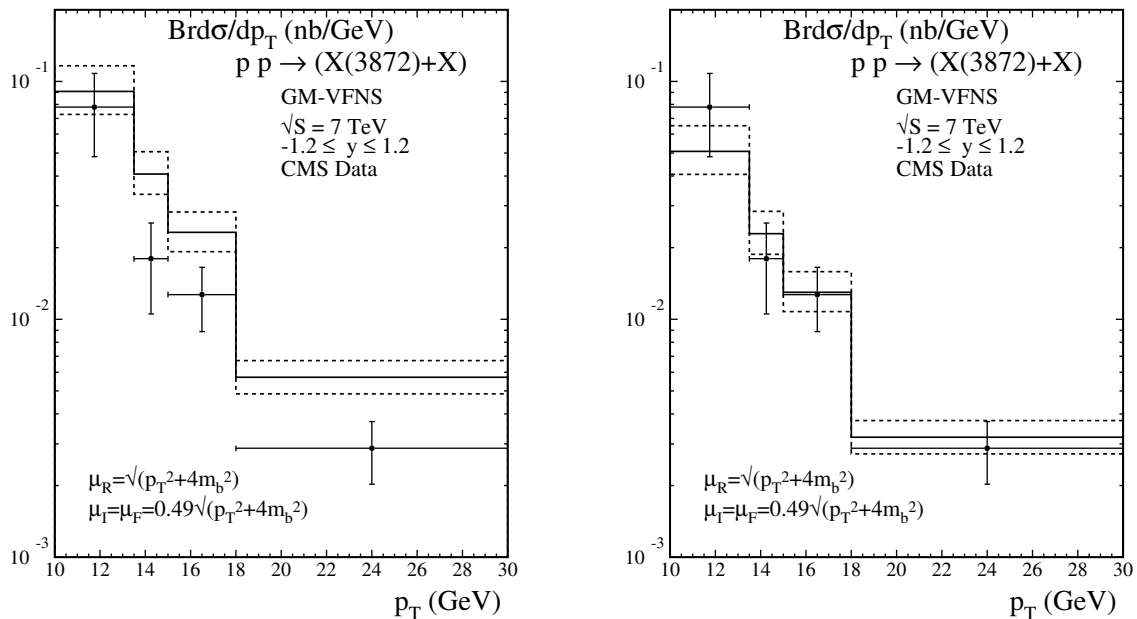


Figure 3: Differential cross sections times branching fractions for  $X(3872)$  non-prompt hadroproduction at  $\sqrt{S} = 7$  TeV, integrated over  $y$  in the region  $|y| \leq 1.2$ , as a function of  $p_T$ . The solid points with error bars are extracted from the CMS data [11]. The solid and the upper and lower dashed histograms represent our NLO GM-VFNS predictions for  $\xi = 1, 0.5, 2$ , respectively. The theoretical predictions were evaluated using the  $R_B$  values in (a) Eq. (3) (left) and (b) Eq. (5) (right).

two standard deviations from the CMS data [11]. It is obvious that there is no room for a discrepancy by a factor between 4 and 8 as claimed in Ref. [12]. The  $\pm 10\%$  uncertainty in the  $R_B$  value in Eq. (3), which is not included in Fig. 3(a), does not affect this conclusion.

In turn, we may now use the CMS data [11] for an independent determination of  $R_B$ , just as we did above with the ATLAS data [12]. We thus find

$$R_B^{\text{CMS}} = \left( 1.89 \pm 0.32 \begin{array}{c} +0.38 \\ -0.33 \end{array} \right) \times 10^{-2}. \quad (5)$$

As expected from Fig. 3(a), this result is smaller than the one in Eq. (3) from the two-lifetime fit in the ATLAS publication [12] and the one in Eq. (4) from matching our  $\psi(2S)$  predictions to the ATLAS  $X(3872)$  data [12]. For a consistency check, we compare the CMS  $X(3872)$  data [11] with our predictions evaluated with the  $R_B$  value fitted to these data in Fig. 3(b), to find good agreement as expected.

We also simultaneously fit  $R_B$  to the non-prompt  $X(3872)$  data from ATLAS [12] and CMS [11]. This is possibly problematic because the experimental (first) errors of  $R_B$  in Eqs. (4) and (5) from the individual fits do not overlap. In other words, the agreement of the underlying ATLAS [12] and CMS [11] data, gauged with respect to our universal NLO GM-VFNS predictions, is marginal. In fact, the combined fit to the  $N = 9$  experimental data points yields a minimum  $\chi^2$  of  $\chi_{\min}^2 = 14.70$ . Following a recommendation by the Particle Data Group [21], we thus rescale the original Gaussian error of 0.24 with the enhancement factor  $\sqrt{\chi_{\min}^2/(N-1)} = 1.36$ . We so obtain

$$R_B^{\text{ATLAS+CMS}} = \left( 2.54 \pm 0.33 \begin{array}{c} +0.49 \\ -0.43 \end{array} \right) \times 10^{-2}, \quad (6)$$

where the theoretical (second) error is determined as in Eqs. (4) and (5).

Finally, it is interesting to compare our results to recent data from the LHCb Collaboration on the dependence on charged-particle multiplicity  $N$  of non-prompt  $\psi(2S)$  and  $X(3872)$  production, with subsequent decays to  $J/\psi\pi^+\pi^-$ , in  $pp$  collisions at  $\sqrt{S} = 8$  TeV [28].<sup>1</sup> The study of the  $X(3872)$  to  $\psi(2S)$  ratio of non-prompt production cross sections as a function of  $N$  may help to shed light on the nature of the exotic  $X(3872)$  state. This ratio, which we identify with  $R_B$ , as we do in this paper, is presented in Fig. 4 in Ref. [28] for five intervals  $[N_{\min}, N_{\max}]$  with weighted centers  $N$ . The results [29] are compiled in Table 1. We observe from Table 1 a slight increase of  $R_B$  with  $N$ , which is, however, not statistically significant. As discussed in Ref. [28], a linear fit to these data points, without considering the correlated systematic uncertainty, gives a positive slope that is consistent with zero within 1.6 standard deviations. For this reason, it appears to be reasonable to fit a horizontal line to these data points. Specifically, we perform three fits using the uncorrelated uncertainties: one to the central data points, and one each to the central data points shifted up and down by their correlated uncertainties. We then take the upward and

<sup>1</sup>In Ref. [28], the  $X(3872)$  hadron is denoted  $\chi_{c1}(2S)$ , an identification that was found to be disfavored through a dedicated NLO NRQCD analysis of prompt  $X(3872)$  hadroproduction [15, 17].

$N_{\min}$	$N_{\max}$	$N$	$R_B \times 10^2$
0	40	30.8	$2.65 \pm 1.32 \pm 0.20$
40	60	50.3	$3.17 \pm 0.60 \pm 0.24$
60	80	69.3	$3.47 \pm 0.71 \pm 0.26$
80	100	88.8	$4.43 \pm 1.20 \pm 0.32$
100	200	118.3	$5.33 \pm 1.59 \pm 0.39$

Table 1:  $R_B$  for five different bins of charged-particle multiplicity  $N$  as measured by the LHCb Collaboration in  $pp$  collisions at  $\sqrt{S} = 8$  TeV. The first and second errors are the uncorrelated and correlated uncertainties, respectively. The data are presented in Fig. 4 of Ref. [28].

downward shifts of the central value to be the error due to the correlated uncertainties, which, in want of the correlation matrix, represents a conservative estimate. This yields

$$R_B^{\text{LHCb}} = (3.48 \pm 0.39 \pm 0.26) \times 10^{-2}, \quad (7)$$

where the first and second errors stem from the uncorrelated and correlated uncertainties, respectively. The fit to the unshifted data points yields a  $\chi^2$  per degree of freedom as low as  $\chi^2/4 = 0.67$ , providing a posteriori a convincing justification for the zero-slope hypothesis. The value in Eq. (7) value is in excellent agreement with the two-lifetime fit from ATLAS [12]. For the reader's convenience, we summarize in Table 2 the various values for  $R_B$  discussed in this paper.

Name	$R_B \times 10^2$	Source
$R_B^{\text{TeV}}$	$18 \pm 8$	Ref. [19]
$R_B^{2L}$	$3.57 \pm 0.348$	ATLAS [12]
$R_B^{\text{LHCb}}$	$3.48 \pm 0.39 \pm 0.26$	extracted from LHCb data [28]
$R_B^{\text{ATLAS}}$	$3.41 \pm 0.37^{+0.63}_{-0.56}$	our fit to ATLAS data [12]
$R_B^{\text{CMS}}$	$1.89 \pm 0.32^{+0.38}_{-0.33}$	our fit to CMS data [11]
$R_B^{\text{ATLAS+CMS}}$	$2.54 \pm 0.33^{+0.49}_{-0.43}$	our joint fit to ATLAS [12] and CMS [11] data

Table 2: Summary of the different  $R_B$  determinations discussed in this article.

### 3 Summary

We updated our prediction of the inclusive cross section of non-prompt  $\psi(2S)$  hadroproduction at NLO in the GM-VFNS [1] and validated it by comparison with ATLAS [12] and

CMS [5] data. From this, we obtained an analogous prediction for non-prompt  $X(3872)$  hadrons by including the appropriate ratio  $R_B$  of branching fractions. In turn, this enabled us to determine  $R_B$  by fitting to ATLAS [12] and CMS [11] data of non-prompt  $X(3872)$  production. This also provided us with a useful test bed to assess determinations of  $R_B$  by other authors. Our findings support the results for  $R_B$  obtained by ATLAS [12] and LHCb [28], which undershoot a previous result [19] by a factor of about 1/5.

## Acknowledgments

We thank J. M. Durham and M. Winn for useful communications regarding Ref. [28] and J. M. Durham for providing us with the data points listed in Table 1 in numerical form. The work of B.A.K was supported in part by the German Federal Ministry for Education and Research BMBF through Grant No. 05H18GUCC1 and by the German Research Foundation DFG through Grants No. KN 365/13-1 and No. KN 365/14-1 within Research Unit FOR 2926 *Next Generation Perturbative QCD for Hadron Structure: Preparing for the Electron-Ion Collider*. The work of I.S. was supported in part by the French National Centre for Scientific Research CNRS through IN2P3 Project GLUE@NLO.

## References

- [1] P. Bolzoni, B. A. Kniehl and G. Kramer, “Inclusive  $J/\psi$  and  $\psi(2S)$  production from  $b$ -hadron decay in  $p\bar{p}$  and  $pp$  collisions,” Phys. Rev. D **88** (2013) 074035 [arXiv:1309.3389 [hep-ph]].
- [2] D. Acosta *et al.* (CDF Collaboration), “Measurement of the  $J/\psi$  meson and  $b$ -hadron production cross sections in  $p\bar{p}$  collisions at  $\sqrt{s} = 1960$  GeV,” Phys. Rev. D **71** (2005) 032001 [arXiv:hep-ex/0412071 [hep-ex]].
- [3] T. Aaltonen *et al.* (CDF Collaboration), “Production of  $\psi(2S)$  mesons in  $p\bar{p}$  collisions at 1.96 TeV,” Phys. Rev. D **80** (2009) 031103(R) [arXiv:0905.1982 [hep-ex]].
- [4] V. Khachatryan *et al.* (CMS Collaboration), “Prompt and non-prompt  $J/\psi$  production in  $pp$  collisions at  $\sqrt{s} = 7$  TeV,” Eur. Phys. J. C **71** (2011) 1575 [arXiv:1011.4193 [hep-ex]].
- [5] S. Chatrchyan *et al.* (CMS Collaboration), “ $J/\psi$  and  $\psi(2S)$  production in  $pp$  collisions at  $\sqrt{s} = 7$  TeV,” JHEP **02** (2012) 011 [arXiv:1111.1557 [hep-ex]].
- [6] R. Aaij *et al.* (LHCb Collaboration), “Measurement of  $J/\psi$  production in  $pp$  collisions at  $\sqrt{s} = 7$  TeV,” Eur. Phys. J. C **71** (2011) 1645 [arXiv:1103.0423 [hep-ex]].

- [7] R. Aaij *et al.* (LHCb Collaboration), “Measurement of  $\psi(2S)$  meson production in  $pp$  collisions at  $\sqrt{s}=7$  TeV,” *Eur. Phys. J. C* **72** (2012) 2100 [Erratum: *Eur. Phys. J. C* **80** (2020) 49] [arXiv:1204.1258 [hep-ex]].
- [8] G. Aad *et al.* (ATLAS Collaboration), “Measurement of the differential cross-sections of inclusive, prompt and non-prompt  $J/\psi$  production in proton–proton collisions at  $\sqrt{s} = 7$  TeV,” *Nucl. Phys. B* **850** (2011) 387 [arXiv:1104.3038 [hep-ex]].
- [9] B. Abelev *et al.* (ALICE Collaboration), “Measurement of prompt  $J/\psi$  and beauty hadron production cross sections at mid-rapidity in  $pp$  collisions at  $\sqrt{s} = 7$  TeV,” *JHEP* **11** (2012) 065 [arXiv:1205.5880 [hep-ex]].
- [10] S. K. Choi *et al.* (Belle Collaboration), “Observation of a Narrow Charmoniumlike State in Exclusive  $B^\pm \rightarrow K^\pm \pi^+ \pi^- J/\psi$  decays,” *Phys. Rev. Lett.* **91** (2003) 262001 [arXiv:hep-ex/0309032 [hep-ex]].
- [11] S. Chatrchyan *et al.* (CMS Collaboration), “Measurement of the  $X(3872)$  production cross section via decays to  $J/\psi \pi^+ \pi^-$  in  $pp$  collisions at  $\sqrt{s} = 7$  TeV,” *JHEP* **04** (2013) 154 [arXiv:1302.3968 [hep-ex]].
- [12] M. Aaboud *et al.* (ATLAS Collaboration), “Measurements of  $\psi(2S)$  and  $X(3872) \rightarrow J/\psi \pi^+ \pi^-$  production in  $pp$  collisions at  $\sqrt{s} = 8$  TeV with the ATLAS detector,” *JHEP* **01** (2017) 117 [arXiv:1610.09303 [hep-ex]].
- [13] A. Ali, J. S. Lange and S. Stone, “Exotics: Heavy pentaquarks and tetraquarks,” *Prog. Part. Nucl. Phys.* **97** (2017) 123 [arXiv:1706.00610 [hep-ph]].
- [14] N. Brambilla, S. Eidelman, C. Hanhart, A. Nefediev, C.-P. Shen, C. E. Thomas, A. Vairo and C.-Z. Yuan, “The  $XYZ$  states: Experimental and theoretical status and perspectives,” *Phys. Rept.* **873** (2020) 1 [arXiv:1907.07583 [hep-ex]].
- [15] M. Butenschoen, Z.-G. He and B. A. Kniehl, “Next-to-leading-order nonrelativistic QCD disfavors the interpretation of  $X(3872)$  as  $\chi_{c1}(2P)$ ,” *Phys. Rev. D* **88** (2013) 011501(R) [arXiv:1303.6524 [hep-ph]].
- [16] C. Meng, H. Han and K.-T. Chao, “ $X(3872)$  and its production at hadron colliders,” *Phys. Rev. D* **96** (2017) 074014 [arXiv:1304.6710 [hep-ph]].
- [17] M. Butenschoen, Z.-G. He and B. A. Kniehl, “Deciphering the  $X(3872)$  via its Polarization in Prompt Production at the CERN LHC,” *Phys. Rev. Lett.* **123** (2019) 032001 [arXiv:1906.08553 [hep-ph]].
- [18] M. Cacciari, S. Frixione, N. Houdeau, M. L. Mangano, P. Nason and G. Ridolfi, “Theoretical predictions for charm and bottom production at the LHC,” *JHEP* **10** (2012) 137 [arXiv:1205.6344 [hep-ph]].

- [19] P. Artoisenet and E. Braaten, “Production of the  $X(3872)$  at the Tevatron and the LHC,” *Phys. Rev. D* **81** (2010) 114018 [arXiv:0911.2016 [hep-ph]].
- [20] G. Bauer (CDF II Collaboration), “The  $X(3872)$  at CDF II,” *Int. J. Mod. Phys. A* **20** (2005) 3765 [arXiv:hep-ex/0409052 [hep-ex]].
- [21] P. A. Zyla *et al.* (Particle Data Group), “Review of Particle Physics,” *Prog. Theor. Exp. Phys.* **2020** (2020) 083C01.
- [22] B. A. Kniehl and G. Kramer, “Inclusive  $J/\psi$  and  $\psi(2S)$  production from  $B$  decay in  $p\bar{p}$  collisions,” *Phys. Rev. D* **60** (1999) 014006 [arXiv:hep-ph/9901348 [hep-ph]].
- [23] I. Helenius and H. Paukkunen, “Revisiting the  $D$ -meson hadroproduction in general-mass variable flavour number scheme,” *JHEP* **05** (2018) 196 [arXiv:1804.03557 [hep-ph]].
- [24] M. Benzke, B. A. Kniehl, G. Kramer, I. Schienbein and H. Spiesberger, “ $B$ -meson production in the general-mass variable-flavour-number scheme and LHC data,” *Eur. Phys. J. C* **79** (2019) 814 [arXiv:1907.12456 [hep-ph]].
- [25] S. Dulat, T.-J. Hou, J. Gao, M. Guzzi, J. Huston, P. Nadolsky, J. Pumplin, C. Schmidt, D. Stump and C.-P. Yuan (CTEQ-TEA Collaboration), “New parton distribution functions from a global analysis of quantum chromodynamics,” *Phys. Rev. D* **93** (2016) 033006 [arXiv:1506.07443 [hep-ph]].
- [26] B. A. Kniehl, G. Kramer, I. Schienbein and H. Spiesberger, “Finite-mass effects on inclusive  $B$ -meson hadroproduction,” *Phys. Rev. D* **77** (2008) 014011 [arXiv:0705.4392 [hep-ph]].
- [27] V. Kartvelishvili (ATLAS Collaboration), private communication.
- [28] R. Aaij *et al.* (LHCb Collaboration), “Observation of multiplicity-dependent prompt  $\chi_{c1}(3872)$  and  $\psi(2S)$  production in  $pp$  collisions,” [arXiv:2009.06619 [hep-ex]].
- [29] J. M. Durham, private communication.